

# Roles of *E. coli* DNA polymerases IV and V in lesion-targeted and untargeted SOS mutagenesis

Mengjia Tang\*, Phuong Pham\*, Xuan Shen\*, John-Stephen Taylor†, Mike O'Donnell‡, Roger Woodgate§ & Myron F. Goodman\*

\* Department of Biological Sciences and Chemistry, University of Southern California, University Park, Los Angeles, California 90089-1340, USA

† Department of Chemistry, Washington University, St. Louis, Missouri 63130, USA

‡ Rockefeller University and Howard Hughes Medical Institute, New York, New York 10021, USA

§ Section on DNA Replication, Repair and Mutagenesis, National Institute of Child Health and Human Development, National Institutes of Health, Bethesda, Maryland 20892-2725, USA

The expression of the *Escherichia coli* DNA polymerases pol V (UmuD'2C complex)<sup>1,2</sup> and pol IV (DinB)<sup>3</sup> increases in response to DNA damage<sup>4</sup>. The induction of pol V is accompanied by a substantial increase in mutations targeted at DNA template lesions in a process called SOS-induced error-prone repair<sup>4</sup>. Here we show that the common DNA template lesions, TT (6–4) photoproducts, TT *cis-syn* photodimers and abasic sites, are efficiently bypassed within 30 seconds by pol V in the presence of activated RecA protein (RecA\*), single-stranded binding protein (SSB) and pol III's processivity  $\beta,\gamma$ -complex. There is no detectable bypass by either pol IV or pol III on this time scale. A mutagenic 'signature' for pol V is its incorporation of guanine opposite the 3'-thymine of a TT (6–4) photoproduct, in agreement with mutational spectra. In contrast, pol III and pol IV incorporate adenine almost exclusively. When copying undamaged DNA, pol V exhibits low fidelity with error rates of around  $10^{-3}$  to  $10^{-4}$ , with pol IV being 5- to 10-fold more accurate. The effects of RecA protein on pol V, and  $\beta,\gamma$ -complex on pol IV, cause a 15,000- and 3,000-fold increase in DNA synthesis efficiency, respectively. However, both polymerases exhibit low processivity, adding 6 to 8 nucleotides before dissociating. Lesion bypass by pol V does not require  $\beta,\gamma$ -complex in the presence of non-hydrolysable ATP $\gamma$ S, indicating that an intact RecA filament may be required for translesion synthesis.

DNA damage in *E. coli* triggers the induction of 'SOS' genes involved in DNA replication, repair and mutagenesis. These genes

are transcriptionally regulated by the LexA repressor protein, with RecA\* acting as a co-protease mediating the self-cleavage and subsequent inactivation of LexA<sup>4</sup>. One facet of the SOS response is a large (~100-fold) increase in the rate of base substitution mutations targeted at template DNA damage sites, in addition to increased untargeted mutations at normal template sites. When pol V (UmuD'2C) is mutated, mutation rates in ultraviolet-irradiated cells drop to spontaneous background levels<sup>5</sup>. In addition to pol V, there are two other LexA-regulated *E. coli* DNA polymerases, pol II<sup>6</sup> and pol IV<sup>3</sup>. Pol IV appears to have little, if any, role in causing damage-induced chromosomal mutations, but does cause mutations on lambda phage<sup>7</sup> and F' episomes<sup>8</sup>. Enigmatic pol II<sup>9</sup> has been shown to be crucial in error-free replication restart<sup>10</sup>. Our focus is on pols IV and V, which are error-prone in distinct ways.

Three common DNA lesions are thymine–thymine pyrimidine (6–4) pyrimidone photoproducts (TT (6–4) photoproducts) and thymine–thymine *cis-syn* cyclobutane photodimers (TT *cis-syn* photodimers) caused by ultraviolet radiation, and apurinic/apyrimidinic (abasic) sites arising from the spontaneous loss of a DNA base, or when glycosylases excise damaged bases or uracil from DNA<sup>11</sup>. Replication *in vivo* is impeded by each lesion<sup>12–14</sup>. We have compared the translesion synthesis (TLS) efficiency and base incorporation specificity of pol V, pol IV and pol III. The forms of the enzymes used were: pol V Mut (or mutasome<sup>15</sup>, consisting of pol V (UmuD'2C), RecA\*,  $\beta,\gamma$ -complex and SSB); pol IV (DinB)<sup>3</sup> with  $\beta,\gamma$ -complex and SSB; and pol III HE (holoenzyme of pol III core,  $\beta,\gamma$ -complex and SSB). Our measurements of TLS show that pol V Mut catalyses efficient bypass of all three lesions within 30 s (Fig. 1). The estimated lesion bypass rates are ~30, 20 and 80% min<sup>-1</sup> for the TT (6–4) photoproduct, TT photodimer and abasic moiety, respectively. No detectable bypass is observed in 30 s using pol III HE or pol IV; the latter shows incorporation opposite each of the lesions but extending no further. After 8 min faint bypass product bands appear for pol III HE and pol IV, with bypass rates of 1.2 and 0.7% min<sup>-1</sup>, respectively, for the TT(6–4) photoproduct, 1 and 0.5% min<sup>-1</sup> for the TT photodimer, and 0.4 and 0.1% min<sup>-1</sup> for the abasic moiety. Extensions from a normal template position (T site, Fig. 1, left gel) are around 88, 98 and 68% at 30 s for pol V Mut, pol III HE and pol IV, respectively. The enzyme levels were chosen to allow similar primer utilization on undamaged DNA templates, with roughly 50% of each primer being extended at 16 min (Fig. 1, left gel). Observations at early times (<2 min) indicate that synthesis by pol III HE is processive, whereas that by pol V Mut or pol IV is much more distributive (Fig. 1).

We used a gel-fidelity assay<sup>16</sup> to measure nucleotide incorporation specificities for pols III, IV and V opposite both positions of a TT

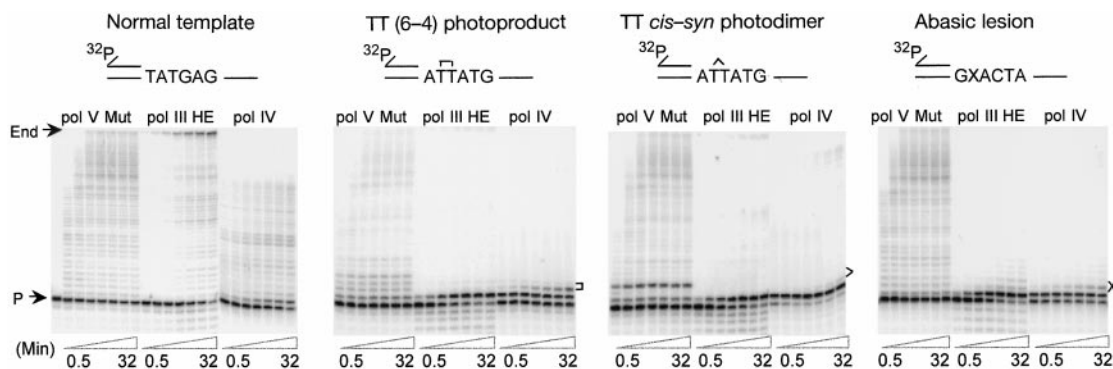


**Figure 1** Comparison of translesion synthesis by pol III HE, pol IV and pol V Mut. Normal and translesion synthesis by pol III core (1 nM), pol IV (25 nM) and pol V (25 nM) were carried out in reactions containing 2 nM primer templates (shown at top), 1 mM ATP, 300 nM SSB, 40 nM  $\beta$ -subunit and 10 nM  $\gamma$ -complex. RecA protein (1  $\mu$ M) was present in pol V reactions to give mutasome, pol V Mut. Reactions were initiated by adding the

polymerase and four dNTPs (100  $\mu$ M each; see Methods). P indicates the location of the non-extended primer. The locations of a TT (6–4) photoproduct, TT *cis-syn* cyclobutane dimer and abasic site are indicated by the square bracket, diagonal bracket and cross, respectively. The lesion bypass rate is calculated as the fraction of primers extended beyond the lesion per min divided by the total amount of primer extended.

(6–4) photoproduct. A <sup>32</sup>P-labelled primer is extended by incorporating a single ‘running-start’ T to reach the 3′-T of a TT (6–4) photoproduct (Fig. 2a). Both pol V Mut and pol IV have no measurable 3′-exonuclease proofreading activity, and pol III α-HE is a proofreading-deficient form of pol III HE.

Mutations occur predominantly at the 3′-T site of a TT (6–4) photoproduct, with 5′-T mutations occurring much less frequently<sup>4</sup>. In accord with this observation, we find that pol V Mut favours incorporation of G over A opposite the 3′-T site by sixfold (Fig. 2a, Table 1). In contrast, pol III α-HE and pol IV favour incorporation of A over G by 27- and 3.3-fold, respectively (Fig. 2a). At the 5′-T, pol V Mut incorporates A about 8- to 13-fold more than G, when either A·T or G·T primer ends are extended (Fig. 2b, Table 1). Incorporation of G is not detectable at the 5′-T site with either pol III α-HE or pol IV (data not shown). Thus, our data for pol V Mut agree qualitatively and quantitatively with *in vivo* mutational data showing increased 3′-T → C transition mutations with a much smaller increase in 5′-T mutations<sup>14,17</sup> (Table 1). The absence of detectable amounts of incorporation of either C or T at either TT site by pol V is consistent with the absence of transversions *in vivo* (data not shown). Similar kinetic analyses performed using a TT *cis-syn* photodimer and an abasic lesion also agree with *in vivo* measurements<sup>13,17,18</sup> (Table 1). We conclude that pol V Mut is probably responsible for SOS mutations targeted to DNA damage

sites, on the basis of its high TLS efficiency and recapitulation of *in vivo* mutational specificity.

An examination of TLS gel bands also reveals the error-prone nature of pol V Mut at undamaged template sites (Fig. 2a). All three polymerases catalysed TLS by incorporating T opposite A and A opposite T at the two template sites immediately downstream from the lesion. However, pol V Mut also formed mismatches at the next template base G (Fig. 2a). These data are consistent with *in vivo* experiments showing that, in addition to mutations targeted specifically at template lesions, there are also untargeted pol V Mut mutations<sup>19</sup>. No such mismatches occurred with either pol IV or pol III α-HE.

We have also measured the fidelity of nucleotide incorporation of the three polymerases on undamaged DNA template sites (Table 2). For pol V Mut, we find error frequencies of 1–5 × 10<sup>-3</sup> for G·T, T·G, G·G, A·G and T·T mismatches; 3–7 × 10<sup>-4</sup> for G·A, C·A, C·T, T·C and A·C mismatches; 7 × 10<sup>-5</sup> for A·A mismatches; and <10<sup>-5</sup> for C·C mismatches. For pol IV, the error frequencies ranged from ~2 × 10<sup>-3</sup> for G·G to 3 × 10<sup>-5</sup> for C·C mismatches. However, the G·G mismatch is unlikely to be caused by direct misincorporation of dGMP opposite G, but rather by dNTP-stabilized misalignment<sup>20</sup> whereby incorporation of G occurs opposite a template C base immediately downstream from G. This is consistent with pol IV's propensity for catalysing -1 frameshift errors<sup>3</sup>. For comparison with pols IV

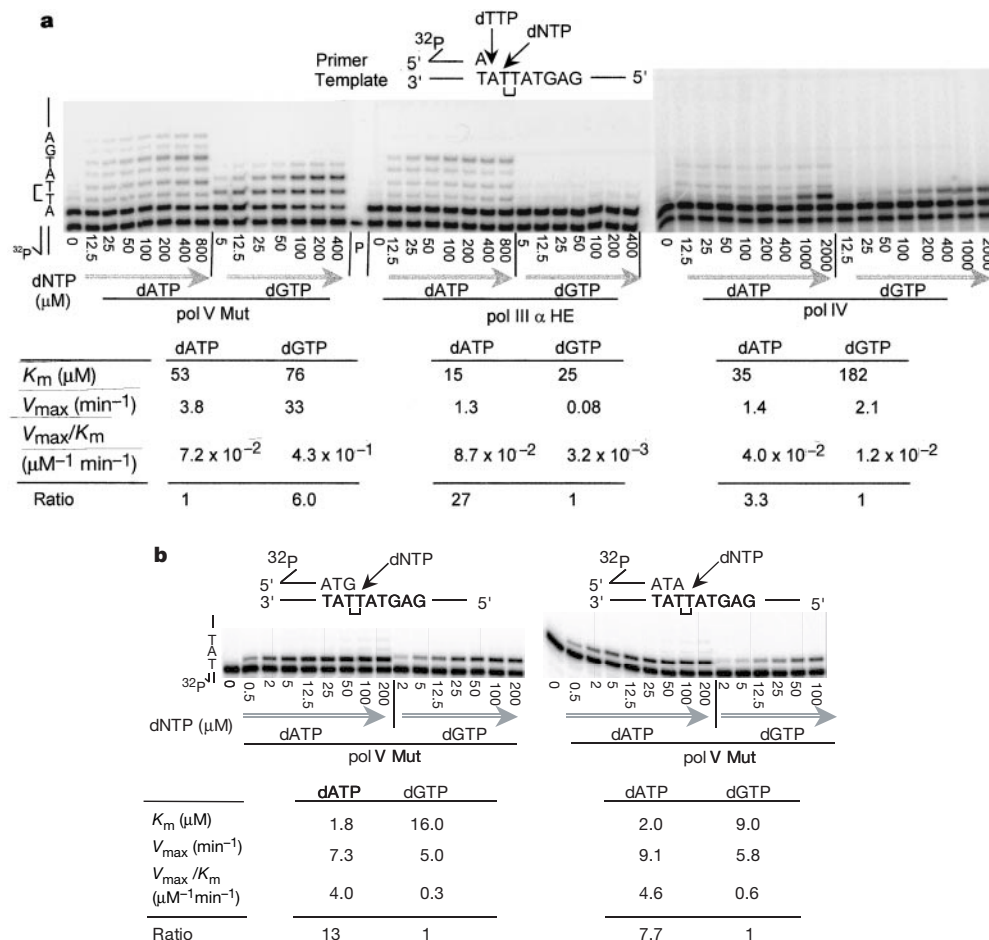


**Figure 2** Incorporation of A compared with G opposite a TT (6–4) photoproduct. **a**, The incorporation kinetics of either A or G were measured opposite the 3′-T site of a TT (6–4) photoproduct using pol V Mut, pol IV or pol III α-HE. To reach the target site, a running-start T (10 μM dTTP) is incorporated opposite A as shown at top. The concentrations of dNTP = dATP or dGTP for incorporation opposite the target site were varied. P indicates the location of the non-extended primer. **b**, The incorporation kinetics of either A or G were

measured opposite the 5′-T of a TT (6–4) photoproduct using pol V Mut to extend a primer terminating with either G (left gel) or A (right gel) situated opposite the 3′-T of the TT (6–4) photoproduct. The kinetic analysis, summarized under Methods, is described in detail in ref. 16. Relative efficiencies of incorporation of dATP versus dGTP (ratios shown at the bottom of the tables) are fold-differences between  $V_{max}/K_m$  for incorporation of dATP compared to dGTP.

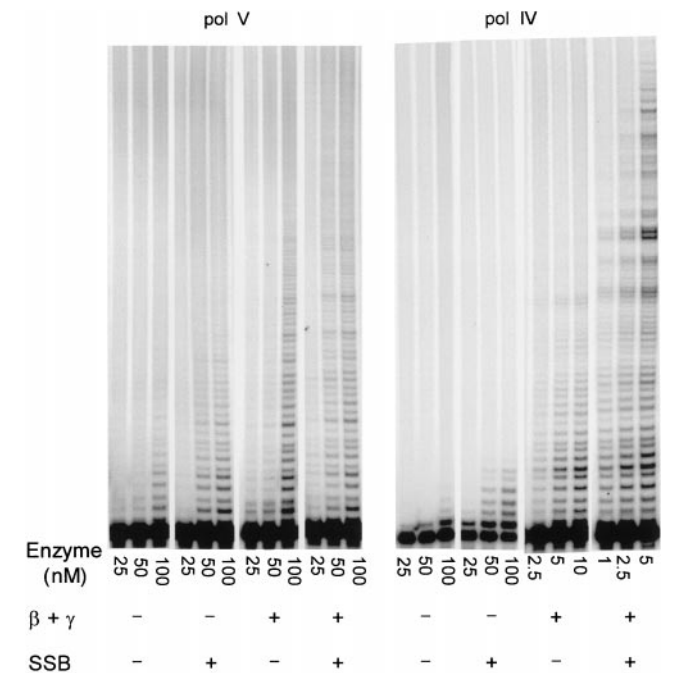


**Figure 3** Analysis of the processivity of pol IV and pol V with or without SSB and  $\beta,\gamma$ -complex. The processivity of pol IV and pol V was measured on circular single-stranded DNA (M13 mp7) primed with a 5'-<sup>32</sup>P-labelled 30-mer (see Methods). Synthesis by pol V was carried out in the presence of RecA protein.

and V Mut, the proofreading-defective pol III  $\alpha$ -HE makes base-substitution errors in the  $10^{-4}$  to  $10^{-6}$  range, consistent with previous measurements<sup>20</sup>. As pols IV and V also exhibit an enhanced ability to extend mismatched primer ends<sup>1,3</sup>, an increase in untargeted mutations is likely to result from the combined effect of a relatively high error rate followed by efficient mismatch extension, which inhibits proofreading.

Synthesis on undamaged DNA templates by either pol V with RecA protein or pol IV alone results in a weak, distributive primer-elongation pattern, which is enhanced by addition of either  $\beta,\gamma$ -complex or SSB (Fig. 3). Synthesis by pol V in the absence of RecA protein,  $\beta,\gamma$ -complex and SSB is weak<sup>2</sup>. Synthesis by pol IV is distributive in the absence of  $\beta,\gamma$ -complex<sup>3</sup> (Fig. 3), and synthesis by pol V is distributive in the absence of RecA (data not shown). Maximal stimulation for both polymerases occurs when  $\beta,\gamma$ -complex and SSB are present simultaneously in the reaction (Fig. 3); but even under the most favourable conditions, processivities are limited to around 6–8 nucleotides for each polymerase. Similar results are obtained in the presence of a heparin trap (data not shown). Whereas RecA strongly stimulates pol V activity on both damaged and undamaged DNA templates and is required for pol V-catalysed TLS *in vitro*<sup>1,2</sup>, it has no measurable effect on pol IV synthetic activity (data not shown).

Most striking, however, are the effects of RecA protein on pol V, and  $\beta,\gamma$ -complex on pol IV. There is a 15,000- and 3,000-fold increase in DNA synthesis efficiency ( $V_{max}/K_m$ ) for pol V and pol IV, respectively (Fig. 4). These increased efficiencies are reflected in marked  $K_m$  reductions for dNTP substrates; the steady-state  $K_m$  values are reduced from 1.2 mM to 0.08  $\mu$ M for pol V and from

**Table 1** Pol V Mut insertion specificity at DNA template lesions: comparing *in vitro* and *in vivo* data

	TT (6–4) photoproduct						TT <i>cis-syn</i> photodimer							
	Opposite 3'T		Opposite 5'T		Opposite 3'T		Opposite 5'T		Abasic lesion					
	<i>In vitro</i> kinetics*	<i>In vivo</i> 1†	2‡	<i>In vitro</i> kinetics	1†	2‡	<i>In vitro</i> kinetics	1§	2‡	<i>In vitro</i> kinetics	<i>In vivo</i>			
A	14.3	11	27	92.2	94	98	98	94	98	95.2	99	98	63.6	54–80
G	85.7	87.5	69	7.8	2	2	2	1		4.8	<1	1	36.4	15–20

\*The data represent the percentage of either A or G incorporated opposite each template lesion site derived from the ratio of A/G incorporation specificity ( $V_{max}/K_m$ ) – see, for example, Fig. 2 for TT (6–4) photoproduct. Incorporation of either T or C opposite each of the lesions is negligible.

† From ref. 14.

‡ From ref. 17.

§ From ref. 18.

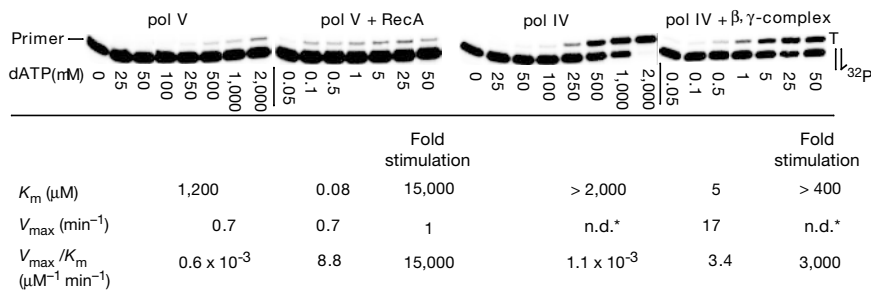
|| From ref. 13.

**Table 2** Fidelity of pol III  $\alpha$  HE, pol IV and pol V Mut by steady state kinetics

dNTP•Template	pol V Mut		pol IV		pol III $\alpha$ -HE	
	$V_{max}/K_m$ ( $\mu$ M <sup>-1</sup> min <sup>-1</sup> )	$f_{inc}^*$	$V_{max}/K_m$ ( $\mu$ M <sup>-1</sup> min <sup>-1</sup> )	$f_{inc}^*$	$V_{max}/K_m$ ( $\mu$ M <sup>-1</sup> min <sup>-1</sup> )	$f_{inc}^*$
dGTP•G	0.23	$2.7 \times 10^{-3}$	0.047	$1.7 \times 10^{-3}$	0.00073	$2.5 \times 10^{-5}$
dATP•G	0.11	$1.3 \times 10^{-3}$	0.018	$6.7 \times 10^{-4}$	0.0029	$1.0 \times 10^{-4}$
dTTP•G	0.41	$4.8 \times 10^{-3}$	0.023	$8.5 \times 10^{-4}$	0.014	$4.8 \times 10^{-4}$
dCTP•G	86	1	27	1	29	1
dGTP•A	0.033	$3.3 \times 10^{-4}$	0.0031	$1.5 \times 10^{-4}$	0.0038	$3.2 \times 10^{-5}$
dATP•A	0.0070	$7.0 \times 10^{-5}$	0.0011	$5.2 \times 10^{-5}$	0.0011	$9.2 \times 10^{-6}$
dTTP•A	100	1	21	1	120	1
dCTP•A	0.055	$5.5 \times 10^{-4}$	0.0020	$9.5 \times 10^{-5}$	0.019	$1.6 \times 10^{-4}$
dGTP•T	0.91	$2.4 \times 10^{-3}$	0.0027	$3.6 \times 10^{-4}$	0.0035	$2.5 \times 10^{-5}$
dATP•T	380	1	7.6	1	140	1
dTTP•T	1.4	$3.7 \times 10^{-3}$	0.00067	$8.8 \times 10^{-5}$	0.017	$1.2 \times 10^{-4}$
dCTP•T	0.31	$8.1 \times 10^{-4}$	0.0017	$2.2 \times 10^{-4}$	0.0069	$4.9 \times 10^{-5}$
dGTP•C	360	1	12	1	56	1
dATP•C	0.19	$5.3 \times 10^{-4}$	0.0016	$1.3 \times 10^{-4}$	0.0040	$7.1 \times 10^{-5}$
dTTP•C	0.26	$7.2 \times 10^{-4}$	0.0017	$1.4 \times 10^{-4}$	0.00029	$5.2 \times 10^{-6}$
dCTP•C	n.d.†	$< 1.0 \times 10^{-5}$	0.00043	$3.6 \times 10^{-5}$	0.00016	$2.9 \times 10^{-6}$

\*The nucleotide misincorporation ratio,  $f_{inc} = (V_{max}/K_m)_W / (V_{max}/K_m)_R$ , where W and R denote incorporation of either a wrong or right nucleotide. The sensitivity of the assay is dependent on polymerase activity, ( $V_{max}/K_m)_R$ , and can detect a larger misincorporation range for pol III  $\alpha$ -HE ( $\sim 10^{-6}$ ) compared to pol V Mut ( $< 10^{-6}$ ). The s.e. values for  $f_{inc}$  are  $\pm 30\%$ .

† n.d., not detected.



\*n.d. refers to 'not determined'

**Figure 4** Effect of RecA and  $\beta, \gamma$ -complex on incorporation of correct dAMP at an undamaged template by pol V and pol IV. Reactions were carried out with undamaged circular ssDNA M13mp7 annealed to a 30-mer  $^{32}\text{P}$ -labelled primer. Synthesis by pol V was performed in the presence of  $\beta, \gamma$ -complex, SSB and ATP. Apparent  $K_m$  and  $V_{max}$  values were obtained by plotting nucleotide incorporation rate against dNTP concentration

>2 mM to 5  $\mu\text{M}$  for pol IV (Fig. 4). In agreement with a previous model<sup>21</sup>, it appears that RecA protein, and to a much lesser extent  $\beta, \gamma$ -complex, serves to target pol V to replication complexes stalled at DNA template lesions. The presence of RecA\* is absolutely required for TLS by pol V<sup>1,2</sup>. However,  $\beta, \gamma$ -complex can be dispensed with *in vitro* when non-hydrolysable ATP $\gamma$ S replaces ATP in the reaction (Fig. 5), indicating that RecA filament disassembly, occurring in the presence of ATP but not ATP $\gamma$ S<sup>22</sup>, may 'extinguish' pol V activity. This result appears to resolve a difference in requirements for pol V-catalysed TLS between our data<sup>1,2</sup> and those of ref. 23, which did not require  $\beta, \gamma$ -complex. In our experiments there is 1 RecA per 5 to 15 nucleotides, compared with a much higher 5 RecA per nucleotide in ref. 23, probably sufficient to maintain an intact RecA filament. Thus RecA may activate pol V while targeting it to a DNA damage site, whereas  $\beta, \gamma$ -complex could help tether pol V at the 3'-primer end during the ATP-driven dynamic RecA assembly-disassembly process. The large (3,000-fold) stimulation of  $\beta, \gamma$ -complex on pol IV activity indicates that processivity proteins might facilitate activation and targeting of pol IV at stalled replication forks on undamaged DNA.

Our *in vitro* data (Table 1) appear to recapitulate qualitatively and quantitatively the *in vivo* requirements of pol V Mut in causing SOS

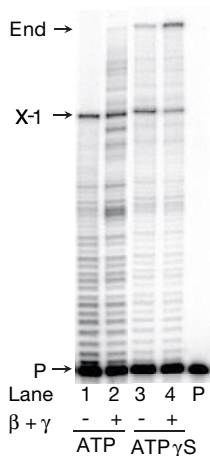


**Figure 5** Role of  $\beta, \gamma$ -complex in abasic site bypass by pol V in the presence of ATP or ATP- $\gamma$ S. All lesion bypass reactions were carried out at 37 °C for 10 min in the presence of 2 nM DNA substrate, RecA protein (1  $\mu\text{M}$ ), SSB (300 nM), pol V (100 nM), 4 dNTPs (100  $\mu\text{M}$ ) and 1 mM of either ATP or ATP- $\gamma$ S.  $\beta$ -subunit and  $\gamma$ -complex, if present, were at 40 nM and 10 nM, respectively. The DNA substrate is a  $^{32}\text{P}$ -labelled primer annealed to a 7.2-kb linear single-stranded DNA with an abasic lesion, as described<sup>15</sup>. The unextended primer P, the upstream site before the lesion (X-1) and the end of template are indicated on the left.

and fitting the data to a saturation curve (rectangular hyperbola) using nonlinear least squares<sup>16</sup>. Note that for pol IV alone, individual  $K_m$  and  $V_{max}$  values could not be measured because the nucleotide incorporation rate remained linear throughout the entire dATP concentration range (0–2,000  $\mu\text{M}$ ); the  $V_{max}/K_m$  value is given by the slope of the line. n.d., not determined.

lesion-targeted mutations. The function of pol V Mut in generating SOS non-targeted chromosomal mutations may be to create genetic diversity during evolution<sup>24</sup>. Proposing a biochemical role for pol IV during the SOS response seems more tenuous. It would be surprising if *E. coli* pol IV, an SOS-induced polymerase with many eukaryotic and prokaryotic DNA repair homologues<sup>25,26</sup>, failed to have a well defined cellular function. Although one can rule out a role for pol IV in SOS-targeted ultraviolet mutagenesis<sup>4</sup>, it nevertheless causes untargeted mutations on phage lambda<sup>7</sup>, and also on an F' plasmid when overproduced<sup>8</sup>. Perhaps pol IV is required to alleviate stalled replication forks on undamaged DNA. Stalling of pol III HE can be caused by mismatched or misaligned primer-ends that cannot be proofread, a suggestion supported by the *in vitro* properties of pol III HE<sup>20</sup>. Thus, error-prone pol IV and pol V may have complementary roles in *E. coli*, with pol IV extending aberrant primer 3'-ends and pol V Mut catalysing TLS. As pol IV and pol V Mut are both poorly processive and dissociate after relieving a blocked replication fork, pol III HE can then replace the errant polymerases to complete chromosomal replication. □

**Methods**

**Materials**

Ultrapure ATP, dNTPs, *E. coli* single-stranded binding protein (SSB) and RecA protein were purchased from Amersham-Pharmacia. Purification of pol III core and its accessory proteins<sup>27</sup> and pol V<sup>2</sup> were carried out as described. For DNA polymerase IV (DinB). The coding sequence of pol IV (DinB) was amplified from genomic *E. coli* DNA and cloned into pMAL-c2x (New England Biolabs) to create a Maltose-binding-protein-DinB overexpression vector. We purified the MBP-DinB fusion protein by amylose affinity chromatography using standard protocols. Fractions containing MBP-DinB were pooled, concentrated and applied to a gel-filtration Superdex 200 XK 26/60 column (Amersham-Pharmacia). The column was developed with buffer A (20 mM Tris-HCl (pH 7.4), 200 mM NaCl, 1 mM EDTA, 1 mM DTT). Fractions containing MBP-DinB (>95% pure) were collected, supplemented with 20% glycerol and aliquots frozen at -70 °C.

**DNA substrates**

Templates used in this study were 7.2-kilobase (kb) linear M13mp7 single-stranded DNA with an abasic site 50 bases from the 5'-end<sup>15</sup>, and a TT (6-4) photoproduct or a TT *cis-syn* photodimer 53 bases from the 5' end. We prepared and characterized the TT lesions as described<sup>28</sup>. 5'- $^{32}\text{P}$ -labelled 30-mers were used as primers. For the measurement of incorporation kinetics opposite an abasic site, the first T (3'-T) of a TT (6-4) photoproduct or a TT *cis-syn* photodimer, primers and templates were annealed, placing the 3'-primer end one base before the lesion site (running-start reaction<sup>16</sup>). To measure incorporation kinetics opposite the second T, the 3'-primer end is situated directly opposite the first T of the lesion (standing-start reaction<sup>16</sup>).

**Nucleotide incorporation kinetics on lesioned and natural DNA primer templates**

All reaction mixtures (10  $\mu\text{l}$ ) contained 20 mM Tris (pH 7.5), 8 mM MgCl<sub>2</sub>, 5 mM DTT, 0.1 mM EDTA, 25 mM sodium glutamate, 1 mM ATP, 40  $\mu\text{g ml}^{-1}$  BSA and 4% (v/v) glycerol. Primer/template DNA (2 nM) was incubated at 37 °C for 2 min at varying dNTP substrate concentrations, 40 nM of  $\beta$ -subunit (as dimer), 10 nM  $\gamma$ -complex, 300 nM SSB (as tetramer) and RecA (1  $\mu\text{M}$ ) (for pol V, but not pol IV). Running-start reactions were initiated by adding 10  $\mu\text{M}$  of a running start dNTP and either pol III  $\alpha$ -subunit (1–5 nM),



pol IV (20 nM) or pol V (25–50 nM). The running-start nucleotide was absent in standing-start reactions. Reactions were run at 37 °C for 5 min and quenched by adding 20 µl of 20 mM EDTA in 95% formamide. Primer–template extension products were heat denatured and run on a 16% polyacrylamide denaturing gel. We measured integrated gel-band intensities by phosphorimaging using ImageQuant software (Molecular Dynamics). Nucleotide incorporation rates opposite both undamaged and lesion target sites were determined, and apparent  $V_{max}/K_m$  values and nucleotide misincorporation frequencies were calculated as described<sup>16</sup>. We carried out fidelity measurements using standing-start reactions on undamaged linear M13mp7 DNA templates annealed to 30mer <sup>32</sup>P-labelled primers with ATP (100 µM). The following template sequences were used: 3'...GTTGC CG...; 3'...CGTAGCC...; 3'TCGTAGC...; 3'TATCAAC, where the base in bold is the template target site at which the nucleotide misincorporation ratio,  $f_{inc}$ , was calculated.

**Processivity measurements**

We measured the processivity of pol IV and pol V Mut on a single-stranded circular DNA (M13 mp7) primed with a 5'-<sup>32</sup>P-labelled 30-mer primer as described<sup>20</sup>. A fixed amount of substrate (10 nM) was incubated with decreasing amounts of pol IV or pol V at 37 °C for 3 min. If indicated, other proteins included in the reactions were: RecA (5 µM), SSB (1.5 µM), β (200 nM) and γ-complex (50 nM). ATP (1 mM) is added in reactions containing RecA and/or γ-complex. Reactions were initiated by adding four dNTPs (100 µM), quenched after 5 min and analysed on a 12% denaturing polyacrylamide gel. Reaction products were quantified by phosphorimaging. Processivities were measured at polymerase concentrations, where product lengths remained stable, and the number of primers used remained less than 10%. We computed processivity as a ratio of the total number of nucleotides added in the reaction to the number of extended DNA primers. High enzyme/DNA ratios are required to carry out primer extension (Fig. 3), probably because the polymerases bind to the long regions of single-stranded DNA. We have previously observed cooperative binding of pol V to single-stranded DNA<sup>20</sup>.

Received 13 December 1999; accepted 4 February 2000.

1. Tang, M. *et al.* Biochemical basis of SOS mutagenesis in *Escherichia coli*: reconstitution of *in vitro* lesion bypass dependent on the UmuD<sub>2</sub>C mutagenic complex and RecA protein. *Proc. Natl Acad. Sci. USA* **95**, 9755–9760 (1998).
2. Tang, M. *et al.* UmuD<sub>2</sub>C is an error-prone DNA polymerase, *Escherichia coli* pol V. *Proc. Natl Acad. Sci. USA* **95**, 8919–8924 (1999).
3. Wagner, J. *et al.* The *dinB* gene encodes a novel *Escherichia coli* DNA polymerase (DNA pol IV). *Mol. Cell* **40**, 281–286 (1999).
4. Friedberg, E. C., Walker, G. C. & Siede, W. *DNA Repair and Mutagenesis* 407–522 (ASM, Washington, 1995).
5. Kato, T. & Shinoura, Y. Isolation and characterization of mutants of *Escherichia coli* deficient in induction of mutagenesis by ultraviolet light. *Mol. Gen. Genet.* **156**, 121–131 (1977).
6. Bonner, C. A., Hays, S., McEntee, K. & Goodman, M. F. DNA polymerase II is encoded by the DNA damage-inducible *dinA* gene of *Escherichia coli*. *Proc. Natl Acad. Sci. USA* **87**, 7663–7667 (1990).
7. Brotocorne-Lannoye, A. & Maenhaut-Michel, G. Role of RecA protein in untargeted UV mutagenesis of bacteriophage λ: Evidence for the requirement for the *dinB* gene. *Proc. Natl Acad. Sci. USA* **83**, 3904–3908 (1986).
8. Kim, S.-R. *et al.* Multiple pathways for SOS-induced mutagenesis in *Escherichia coli*: An over-expression of *dinB/dinP* results in strongly enhancing mutagenesis in the absence of any exogenous treatment to damage DNA. *Proc. Natl Acad. Sci. USA* **94**, 13792–13797 (1997).
9. Knippers, R. DNA polymerase II. *Nature* **228**, 1050–1053 (1970).
10. Rangarajan, S., Woodgate, R. & Goodman, M. F. A phenotype for enigmatic DNA polymerase II: a pivotal role for pol II in replication restart in UV-irradiated *Escherichia coli*. *Proc. Natl Acad. Sci. USA* **96**, 9224–9229 (1999).
11. Lindahl, T. DNA repair enzymes. *Annu. Rev. Biochem.* **51**, 61–87 (1982).
12. Banerjee, S. K., Christensen, R. B., Lawrence, C. W. & LeClerc, J. E. Frequency and spectrum of mutations produced by a single *cis-syn* thymine–thymine cyclobutane dimer in a single-stranded vector. *Proc. Natl Acad. Sci. USA* **85**, 8141–8145 (1988).
13. Lawrence, C. W., Borden, A., Banerjee, S. K. & LeClerc, J. E. Mutation frequency and spectrum resulting from a single abasic site in a single-stranded vector. *Nucleic Acids Res.* **18**, 2153–2157 (1990).
14. LeClerc, J. E., Borden, A. & Lawrence, C. W. The thymine–thymine pyrimidine–pyrimidone(6–4) ultravioletlight photoproduct is highly mutagenic and specifically induces 3' thymine-to-cytosine transitions in *Escherichia coli*. *Proc. Natl Acad. Sci. USA* **88**, 9685–9689 (1991).
15. Rajagopalan, M. *et al.* Activity of the purified mutagenesis proteins UmuC, UmuD', and RecA in replicative bypass of an abasic DNA lesions by DNA polymerase III. *Proc. Natl Acad. Sci. USA* **89**, 10777–10781 (1992).
16. Creighton, S., Bloom, L. B. & Goodman, M. F. In *Methods Enzymol.* Vol. 262 (ed. Campbell, J. L.) 232–256 (Academic, San Diego, 1995).
17. Smith, C. A. *et al.* Mutation spectra of M13 vectors containing site-specific *cis-syn*, *trans-syn-I*, (6–4), and dewar pyrimidone photoproducts of thymidyl-(3'→5')-thymidine in *Escherichia coli* under SOS conditions. *Biochemistry* **35**, 4146–4154 (1996).
18. Lawrence, C. W., Banerjee, S. K., Borden, A. & LeClerc, J. E. T–T Cyclobutane dimers are misinstructive, rather than non-instructive, mutagenic lesions. *Mol. Gen. Genet.* **166**, 166–168 (1990).
19. Fijalkowska, I. J., Dunn, R. L. & Schaaper, R. M. Genetic requirements and mutational specificity of the *Escherichia coli* SOS mutator activity. *J. Bacteriol.* **179**, 7435–7445 (1997).
20. Bloom, L. B. *et al.* Fidelity of *Escherichia coli* DNA polymerase III holoenzyme: The effects of β, γ complex processivity proteins and ε proofreading exonuclease on nucleotide misincorporation efficiencies. *J. Biol. Chem.* **272**, 27919–27930 (1997).
21. Sommer, S., Boudsocq, F., Devoret, R. & Bailone, A. Specific RecA amino acid changes affect RecA-UmuD' interaction. *Mol. Microbiol.* **28**, 281–291 (1998).
22. Menetski, J. P. & Kowalczykowski, S. C. Interaction of RecA protein with single-stranded DNA: Quantitative aspects of binding affinity modulation by nucleotide cofactors. *J. Mol. Biol.* **181**, 281–295 (1985).
23. Reuven, N. B., Arad, G., Maor-Shoshani, A. & Livneh, Z. The mutagenic protein UmuC is a DNA

- polymerase activated by UmuD', RecA, and SSB and is specialized for translesion replication. *J. Biol. Chem.* **274**, 31763–31766 (1999).
24. Radman, M. Enzymes of evolutionary change. *Nature* **401**, 866–869 (1999).
25. McDonald, J. P. *et al.* Novel human and mouse homologs of *Saccharomyces cerevisiae* DNA polymerase η. *Genomics* **60**, 20–30 (1999).
26. Gerlach, V. L. *et al.* Human and mouse homologs of *Escherichia coli* DinB (DNA polymerase IV), members of the UmuC/DinB superfamily. *Proc. Natl Acad. Sci. USA* **96**, 11922–11927 (1999).
27. Naktinis, V., Turner, J. & O'Donnell, M. A molecular switch in a replication machine defined by an internal competition for protein rings. *Cell* **84**, 137–145 (1996).
28. Jing, Y., Kao, J. F.-L. & Taylor, J.-S. Thermodynamic and base-pairing studies of matched and mismatched DNA dodecamer duplexes containing *cis-syn*, (6–4) and Dewar photoproducts of TT. *Nucleic Acids Res.* **26**, 3845–3853 (1998).
29. Bambara, R. A., Fay, P. J. & Mallaber, L. M. Methods of analyzing processivity. *Methods Enzymol.* **262**, 270–280 (1995).
30. Bruck, L., Woodgate, R., McEntee, K. & Goodman, M. F. Purification of a soluble UmuD' C complex from *Escherichia coli*. Cooperative binding of UmuD' C to single-stranded DNA. *J. Biol. Chem.* **271**, 10767–10774 (1996).

**Acknowledgements**

This work was supported by National Institutes of Health grants to M.F.G., M.O. and J.-S.T.).

Correspondence and requests for materials should be addressed to M.F.G. (e-mail: mgoodman@mizar.usc.edu).

**Retrotransposition of a bacterial group II intron**

**Benoit Cousineau, Stacey Lawrence, Dorie Smith & Marlene Belfort**

*Molecular Genetics Program, Wadsworth Center, New York State Department of Health, and School of Public Health, State University of New York at Albany, PO Box 22002, Albany, New York 12201-2002, USA*

Self-splicing group II introns may be the evolutionary progenitors of eukaryotic spliceosomal introns<sup>1–7</sup>, but the route by which they invade new chromosomal sites is unknown. To address the mechanism by which group II introns are disseminated, we have studied the bacterial Ll.LtrB intron from *Lactococcus lactis*<sup>8</sup>. The protein product of this intron, LtrA, possesses maturase, reverse transcriptase and endonuclease enzymatic activities<sup>9–11</sup>. Together with the intron, LtrA forms a ribonucleoprotein (RNP) complex which mediates a process known as retrohoming<sup>11</sup>. In retrohoming, the intron reverse splices into a cognate intronless DNA site. Integration of a DNA copy of the intron is recombinase independent but requires all three activities of LtrA<sup>11</sup>. Here we report the first experimental demonstration of a group II intron invading ectopic chromosomal sites, which occurs by a distinct retrotransposition mechanism. This retrotransposition process is endonuclease-independent and recombinase-dependent, and is likely to involve reverse splicing of the intron RNA into cellular RNA targets. These retrotranspositions suggest a mechanism by which spliceosomal introns may have become widely dispersed.

The group II intron donor in these experiments is a twintron/Kan<sup>R</sup> variant of Ll.LtrB, carrying the self-splicing group I *td* intron and a kanamycin resistance (Kan<sup>R</sup>) gene (Fig. 1a, b)<sup>11</sup>. The Kan<sup>R</sup> marker facilitates selection of group II intron mobility events. The group I intron allows identification of those mobility events that have proceeded through an RNA intermediate and in which the group I intron has therefore been lost. The donor was first tested for retrohoming using *L. lactis* and a two-plasmid system with a recipient plasmid containing the cognate Ll.LtrB homing site (Fig. 1a)<sup>11</sup>. After RNP expression under the control of a nis-inducible promoter<sup>12</sup>, inheritance of the Kan<sup>R</sup>-marked intron occurred at 40% or 58% per recipient in two different wild-type hosts (Fig. 1c, crosses 1 and 3, H%). Of these homing products, 98%